Data Reduction Protocols– Isotope Ratio Measurements

Antonio Simonetti
University of Notre Dame

Possible Issues with (LA)-MC-ICP-MS Analyses?

- Precision and accuracy on individual isotopic measurements suffer due to matrix effects and isobaric interferences?
- Availability of suitable reference materials, in relation to matrix-matching in studies of mass-dependent isotopic fractionation, and laser-induced isotopic fractionation
- Factors that contribute to the **accuracy** and **precision** of in-situ measurements-
  - Interplay related to ***sample***, ***laser operating conditions*** and ***processes in the mass spectrometer***

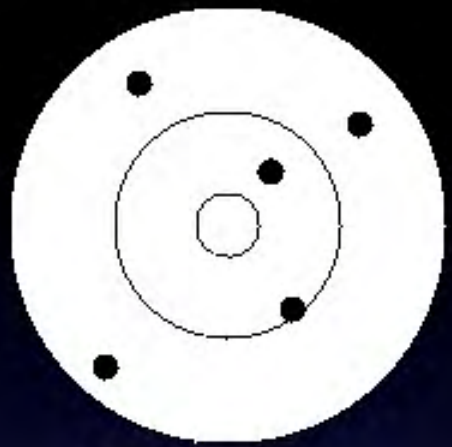

Not accurate
Not precise

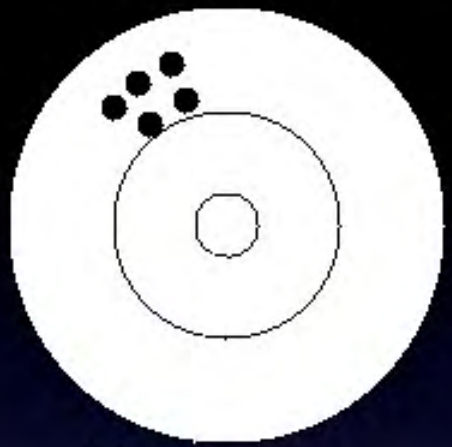

Not accurate
Precise

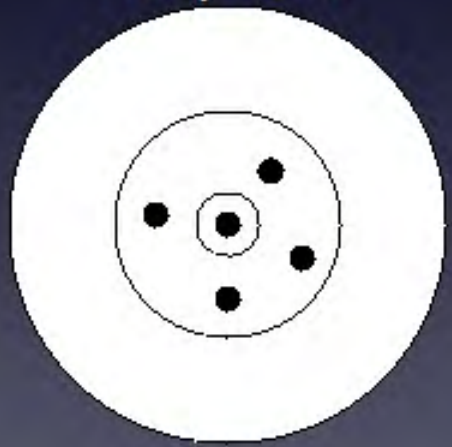

Accurate
Not precise

Accurate
Precise

Parameters affecting accuracy and precision

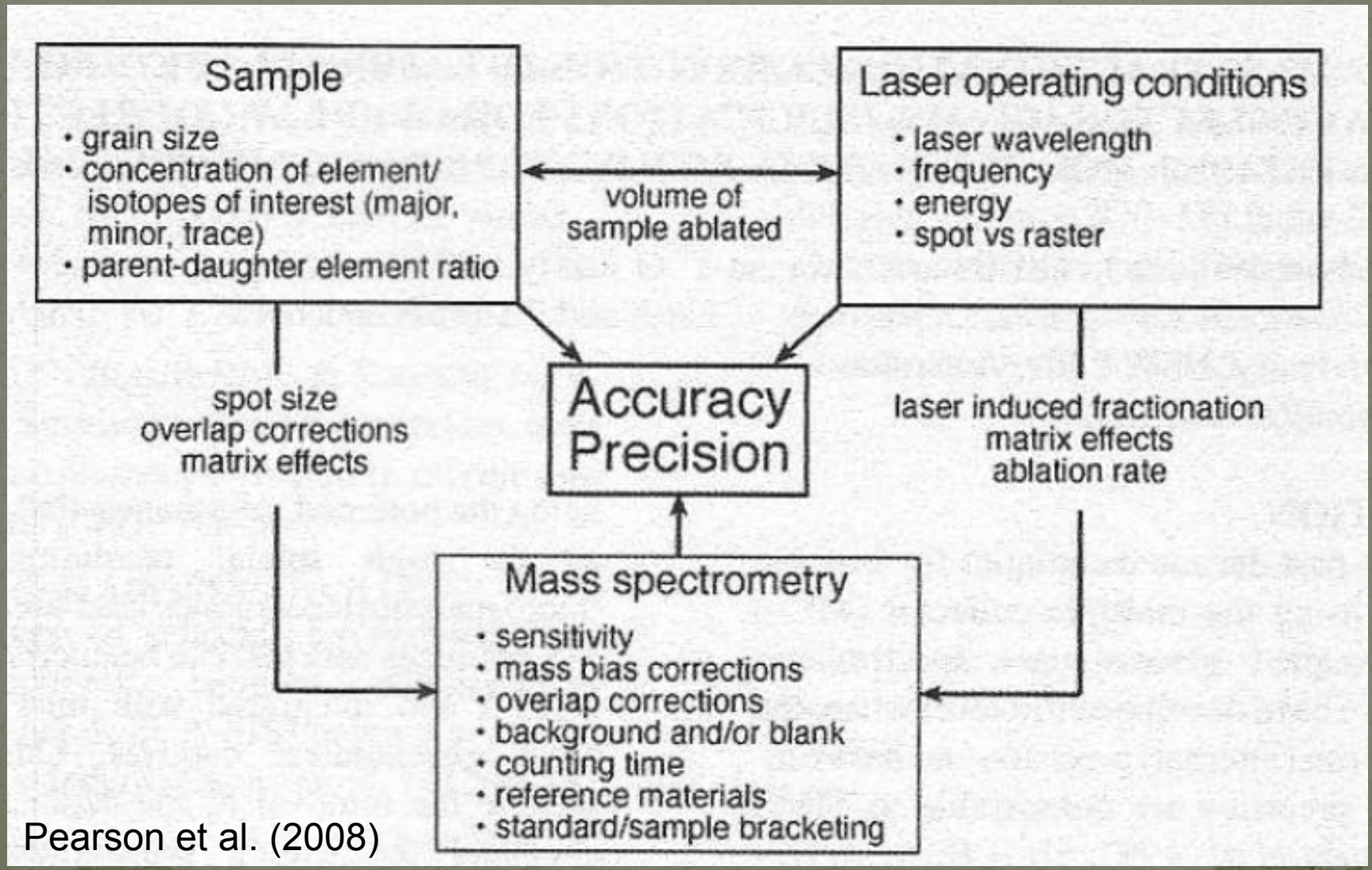

Pearson et al. (2008)

In-situ Isotope Studies

- Fall into 2 groups:
  - Measurement of radiogenic isotopes for trace elements in common rock-forming minerals; e.g., Sr in clinopyroxene, carbonate, feldspar; Hf in zircon; Pb in feldspar, clinopyroxene
  - Study of mass-dependent isotopic fractionation of elements that are major constituents in minerals of interest; e.g., Cu in chalcopyrite, Fe in pyrite

Decision-making time…..

- Size of mineral grain and sensitivity of mass spectrometer will dictate the ***sampling strategy***
- Use '***rastering***' so as to maximize volume of sample ablated and therefore improve precision (i.e. higher ion signal) and 'homogenize' the sample
- Use '***stationary***' analysis, mimic a microprobe and hence attempt to decipher internal variations combined with trace element data, images, etc

Instrumental Mass Bias

- Probably is the most important factor affecting the **accuracy** and **external precision**
- Mass bias is isotopic fractionation (i.e. **artificial change in isotope ratios**) produced by variable transmission of the ion beam in mass spectrometer
- In the MC-ICP-MS instrument, this occurs primarily in the ***plasma*** and ***interface*** regions

Instrumental Mass Bias

- For MC-ICP-MS instruments,
  - The ‘measured’ isotope ratio > the ‘true’ ratio
  - E.g., measured $^{87}Sr/^{86}Sr_{sample}$ > ‘true’ $^{87}Sr/^{86}Sr_{sample}$
- For TIMS (thermal ionization mass spectrometers) instruments,
  - The ‘measured’ isotope ratio < the ‘true’ ratio
  - E.g., measured $^{87}Sr/^{86}Sr_{sample}$ < true $^{87}Sr/^{86}Sr_{sample}$

Instrumental Mass Bias

- In-situ analyses are also affected by the "matrix" of the samples, which may produce isotopic interferences (**isobaric** and **molecular** overlaps) – these also need to be corrected (if possible)!

- Isobaric (equivalent atomic mass) interferences in radiogenic isotope systems include:
  - $^{87}Rb \rightarrow {}^{87}Sr$
  - $^{144}Sm \rightarrow {}^{144}Nd$
  - $^{176}Lu \rightarrow {}^{176}Hf$

Instrumental Mass Bias

- For example, matrix-based molecular interferences include:
  - $^{40}Ca + {}^{31}P + {}^{16}O$ = mass 87 = ^{87}Sr
- The principal inorganic component of enamel is **Hydroxyapatite - $3Ca_3(PO_4)_2.CaX$** [where X can represent a mixture of F, Cl, CO_2, OH]
- In-situ LA-MC-ICP-MS analyses of fossilized teeth from human remains for their Sr isotope composition (Simonetti et al., 2008)
- Tracing migration patterns for ancient civilizations

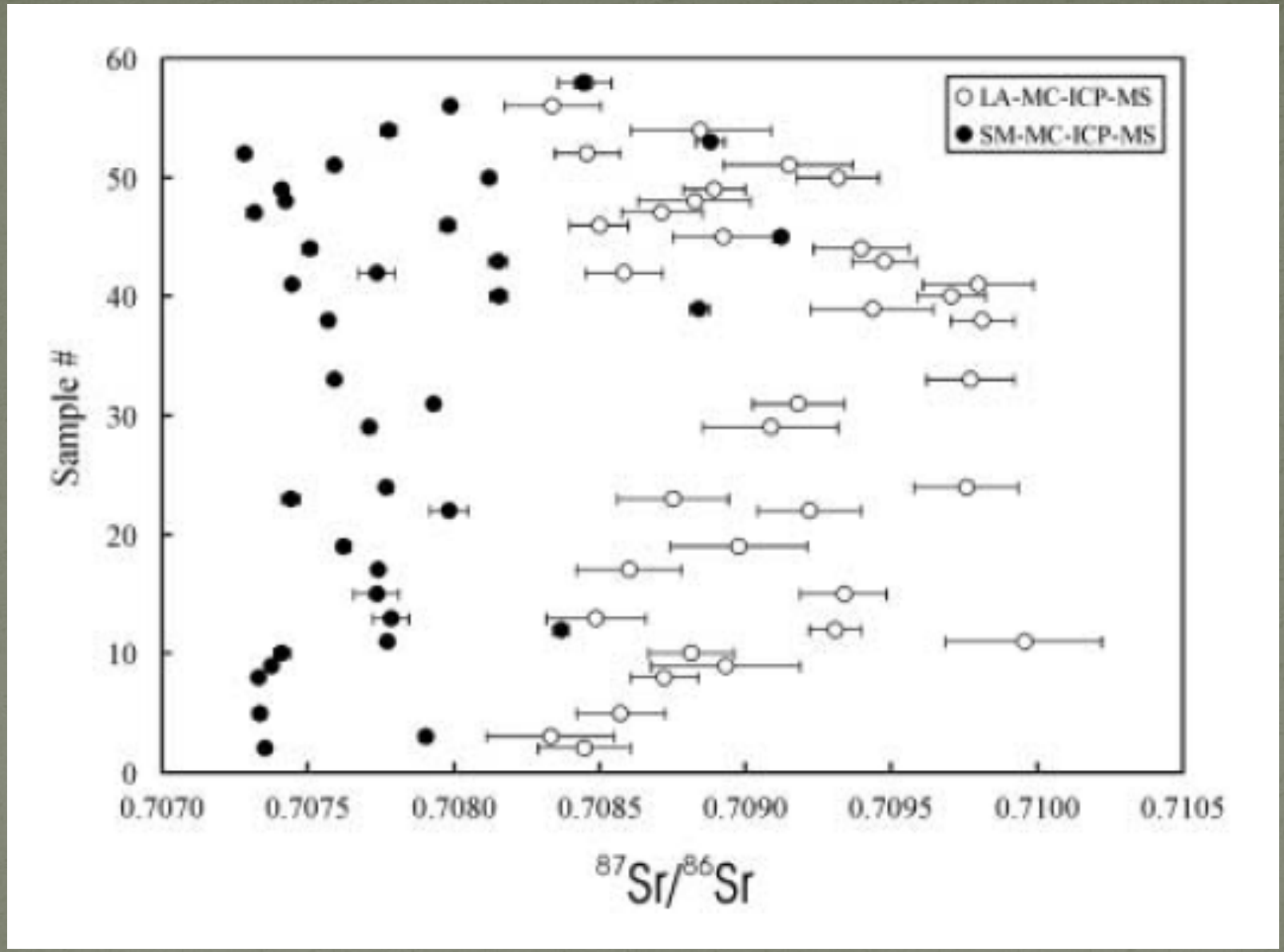

Simonetti et al. (2008, Archaeometry)

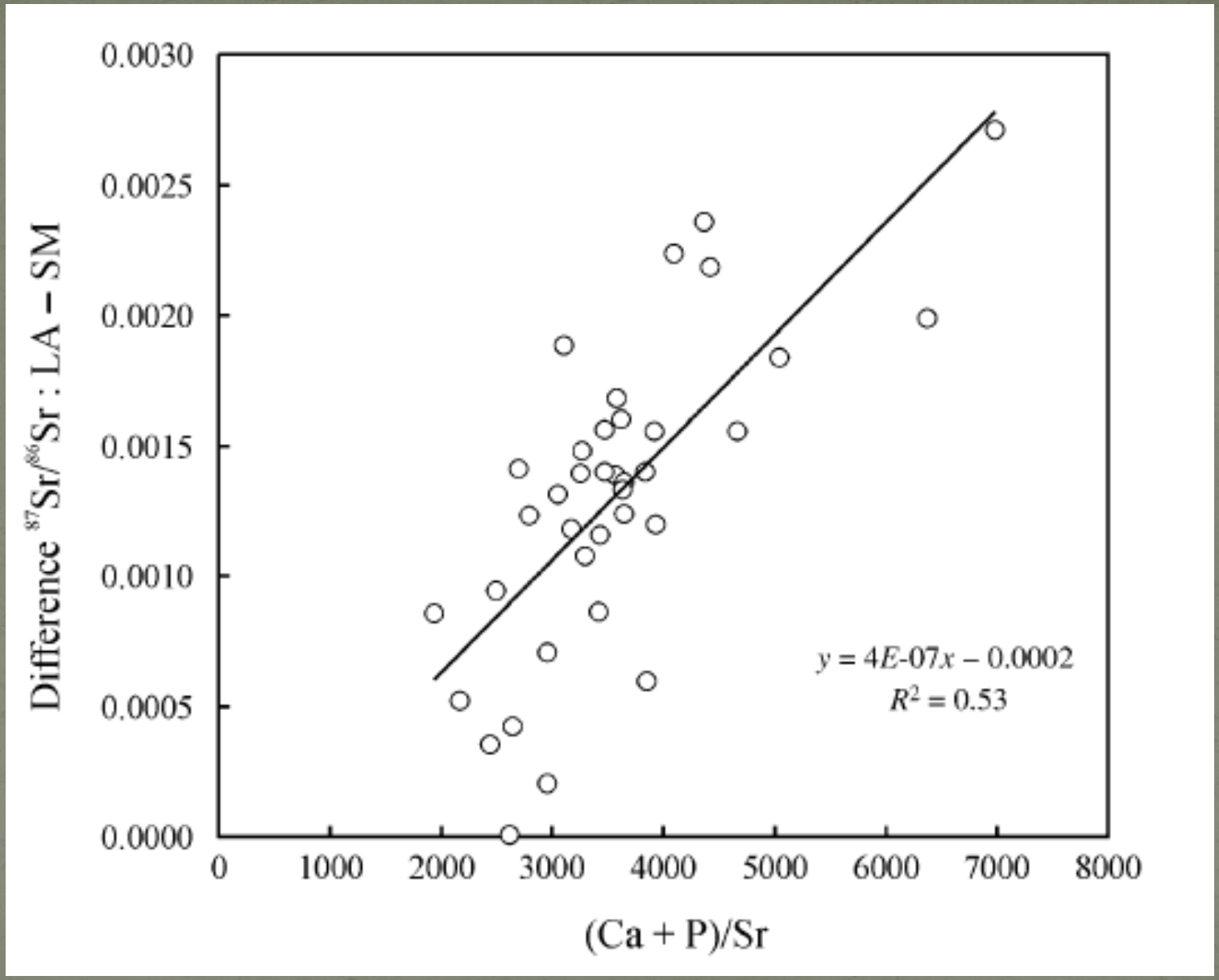

Simonetti et al. (2008, Archaeometry)

Instrumental Mass Bias – The Basics

- Magnitude (i.e., deviation of measured ratio compared to the 'true' value) of mass bias for MC-ICP-MS instrument is larger than that associated with TIMS (thermal ionization mass spectrometry)

- However, the same fractionation laws are applied to correct for instrumental mass bias

Instrumental Mass Bias

- Previous studies have shown that instrumental mass bias can be corrected using a "***generalized power law***"
  - $R_{true} = R_{meas} \bullet f^{(M_2 - M_1)}$
- R_{true} = true isotope ratio of the two isotopes of mass M_1 and M_2 (M_2/M_1)
- R_{meas} = is the isotope ratio (M_2/M_1) measured by the mass spectrometer
  - f = mass fractionation coefficient

Instrumental Mass Bias

- Equation can be rewritten into "***Exponential Law***" form:

$$R_{true} = R_{meas} \bullet (M_2 / M_1)^{f}$$

Instrumental Mass Bias – *Internal Normalization*

- Correction of instrumental mass bias is best achieved by "**internal normalization**"
  - Mass fractionation coefficient (f) can be determined using a pair of stable isotopes with a known or "true" isotopic ratio
  - E.g.,
    - $^{86}Sr/^{88}Sr = 0.1194$
    - $^{146}Nd/^{144}Nd = 0.7219$
    - $^{179}Hf/^{177}Hf = 0.7325$
    - $^{205}Tl/^{203}Tl = 2.3871$

Nu Plasma II - Collector Configuration

	-14	-13	-12	-11	-10	-9	-8	-7	-6	-5	-4	-3	-2	-1	0	1	2	3	4	5	6	7	8	9	10	11	12
	X	F	F	X	F	X	F	X	F	F	F	F	F	F	F	F	F	F	F	F	IC0	IC1	IC2	X	IC3	X	IC4
																					Filter		Filter				
		1	2	2	3		4		5	6	7	8	9	10	11	12	13	14	15	16							
U I																			U238		U236	U235	U234				
U II																	U238			U235	U234	U233					
Th I																			Th232		Th230	Th229					
U/Th/Pb		U238					Th232														Pb208	Pb207	Pb206		Pb204		Hg202
Pb (Hg, Tl)															Pb208	Pb207	Pb206	Tl205	Pb204	Tl203	Hg202						
Pb (Hg)																	Pb208	Pb207	Pb206		Pb204		Hg202				
Hg(Tl,Pb)							Pb207		Tl205	Hg204	Tl203	Hg202	Hg201	Hg200	Hg199	Hg198	Hg197	Hg196	Pt195								
Hg(Pt,Pb)									Pb206		Hg204		Hg202	Hg201	Hg200	Hg199	Hg198	Hg197	Hg196	Pt195							
Os (W,Re,Pt)							Pt194		Os192		Os190	Os189	Os188	Os187	Os186	Re185	Os184		W182								
W(Hf,Os,Ta)									Os188		W186			W183	W182	Ta181	W180	Hf179	Hf178								
Hf(Yb,Lu,W)									W182	Ta181	Hf180	Hf179	Hf178	Hf177	Hf176	Lu175	Hf174	Yb173	Yb172	Yb171							
Lu/Er(Hf,Yb)									177Hf	Lu176	Lu175		Yb173	Yb172					Er167	Er166							
Gd (Dy,Sm)					Dy162		Gd160		Gd158	Gd157	Gd156	Gd155	Gd154		Gd152			Sm149									
Nd(Sm,Ce)									Nd150		Nd148	Sm147	Nd146	Nd145	Nd144	Nd143	Nd142		Ce140								
Ce(Nd,La,Ba,Xe)					Nd146				Ce142		Ce140	La139	Ce138	Ba137	Ce136	Ba135				Xe131							
Ba (Xe,La,Ce)											Ce140	La139	Ba138	Ba137	Ba136	Ba135	Ba134		Ba132	Xe131							
Pd(Ru,Cd,Ag)										Cd111	Pd110	Ag109	Pd108	Ag107	Pd106	Pd105	Pd104		Pd102	Ru101							
Ru(Mo,Pd)			Pd104				Ru102		Ru101		Ru100		Ru99		Ru98		Mo97		Ru96								
Mo(Zr,Ru)			Mo100		Ru99		Mo98		Mo97		Mo96		Mo95		Mo94				Mo92		Zr91						
Zr(Mo,Ru)							Zr96		Mo95		Zr94				Zr92		Zr91		Zr90								
Sr (Rb, Kr)							Sr88		Sr87		Sr86		Rb85		Sr84		Kr83										
Se (Ge, Kr)			Se82				Se80				Se78		Se77		Se76				Se74		Ge73						
Ge (Se)					Se77		Ge76				Ge74		Ge73		Ge72				Ge70								
Zn(Cu,Ni,Ge)			Zn70		Zn69		Zn68		Zn67		Zn66		Cu65		Zn64		Cu63		Ni62								
Cu												Cu65						Cu63									
Cl											Cl37								Cl35								
B					B11															B10							
C					C13															C12							
LI			LI7																	LI6							
Mg							Mg25						Mg25						Mg24								
Si							Si30						Si29						Si28								
S							S34						S33						S32								
Fe(Cr) I		Ni60					Fe56			Fe57			Fe54						Fe54			Cr53					
Fe(Cr) II				Fe58			Fe57			Fe56						Fe54			Cr53								
Ni(Fe)				Ni62			Ni61			Ni60						Ni58			Fe57								
Cr (V,Ti)							Cr54			Cr53			Cr52			Cr51			Cr50			Ti49					

$$R_{true} = R_{meas} \bullet (M_2 / M_1)^{f}$$

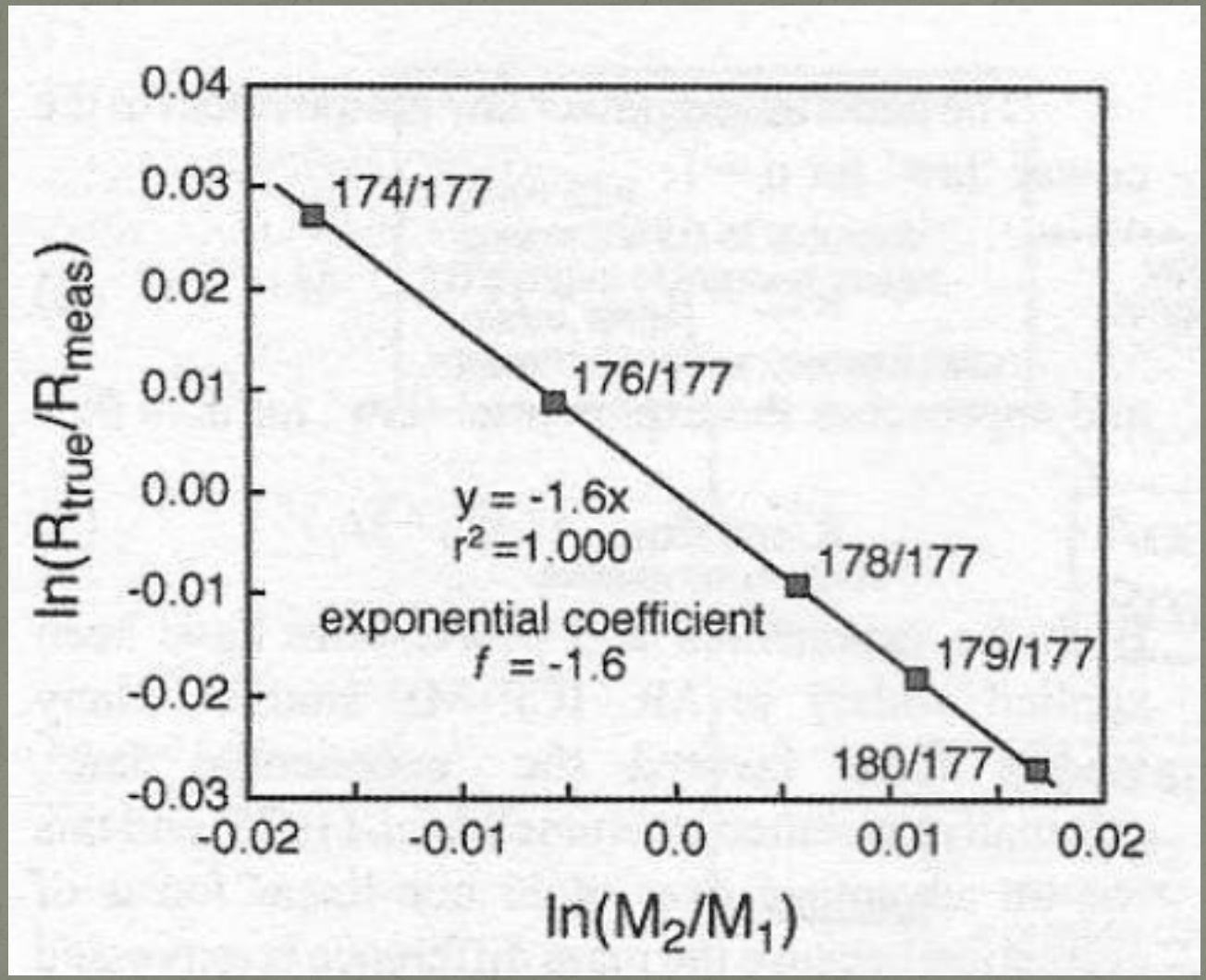

Pearson et al. (2008)

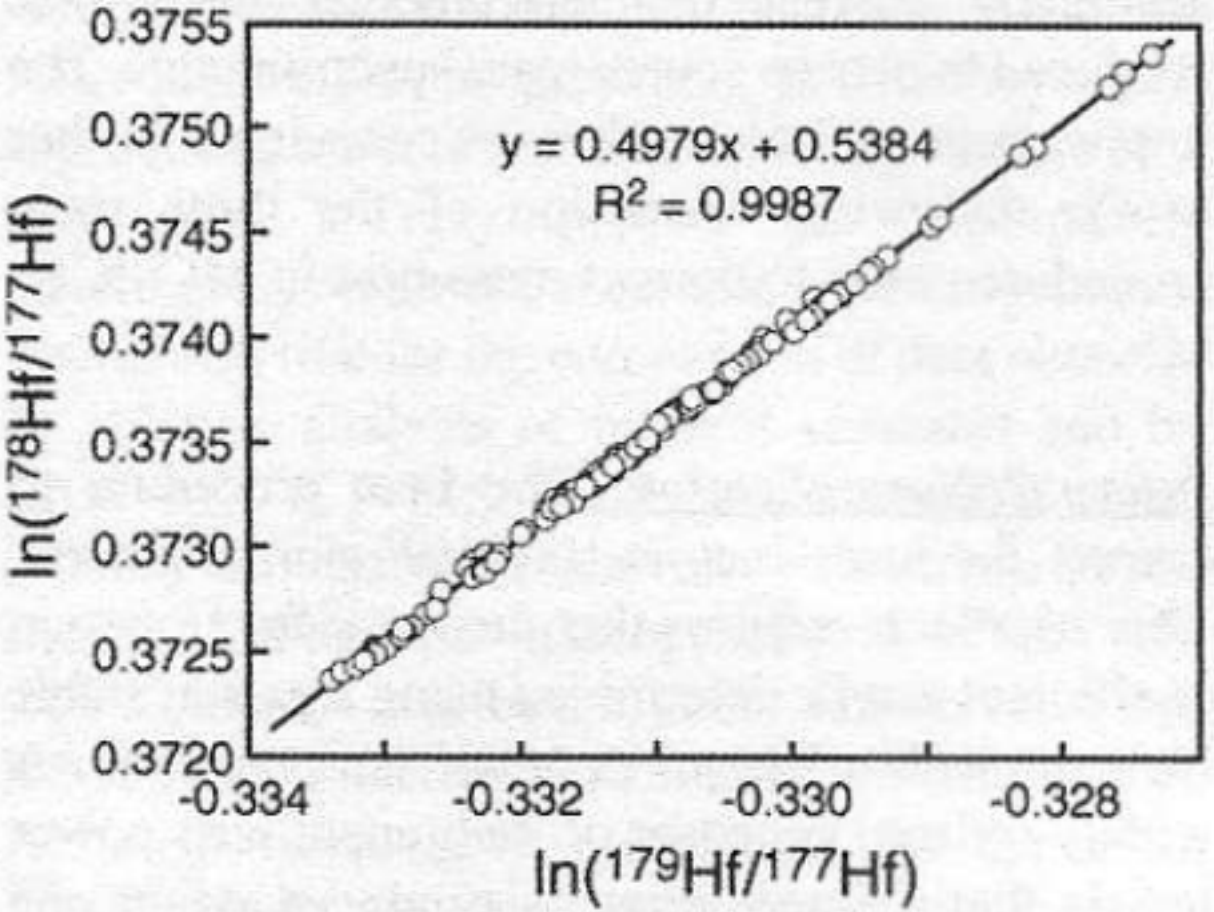

FIG. 7-3. Plot of $\ln(^{178}Hf/^{177}Hf)$ *vs.* $\ln(^{179}Hf/^{177}Hf)$ for the JMC475 Hf solution. The data points are from 132 analyses over a period of 5 years and show the long-term robustness of the instrumental mass fractionation on the Nu Plasma.

Pearson et al. (2008)

Instrumental Mass Bias – *External Correction*

- Linear relationship on log-log plots also holds for when isotope ratios of different elements are plotted, which formed the basis for the '***external***' or '***doped***' correction procedure.

- This technique has been successfully applied to a number of applications as shown by previous investigations
  - Cu-Zn (e.g., Maréchal et al., 1999)
  - Pb-Tl (e.g., Belshaw et al., 1998; Woodhead, 2002)

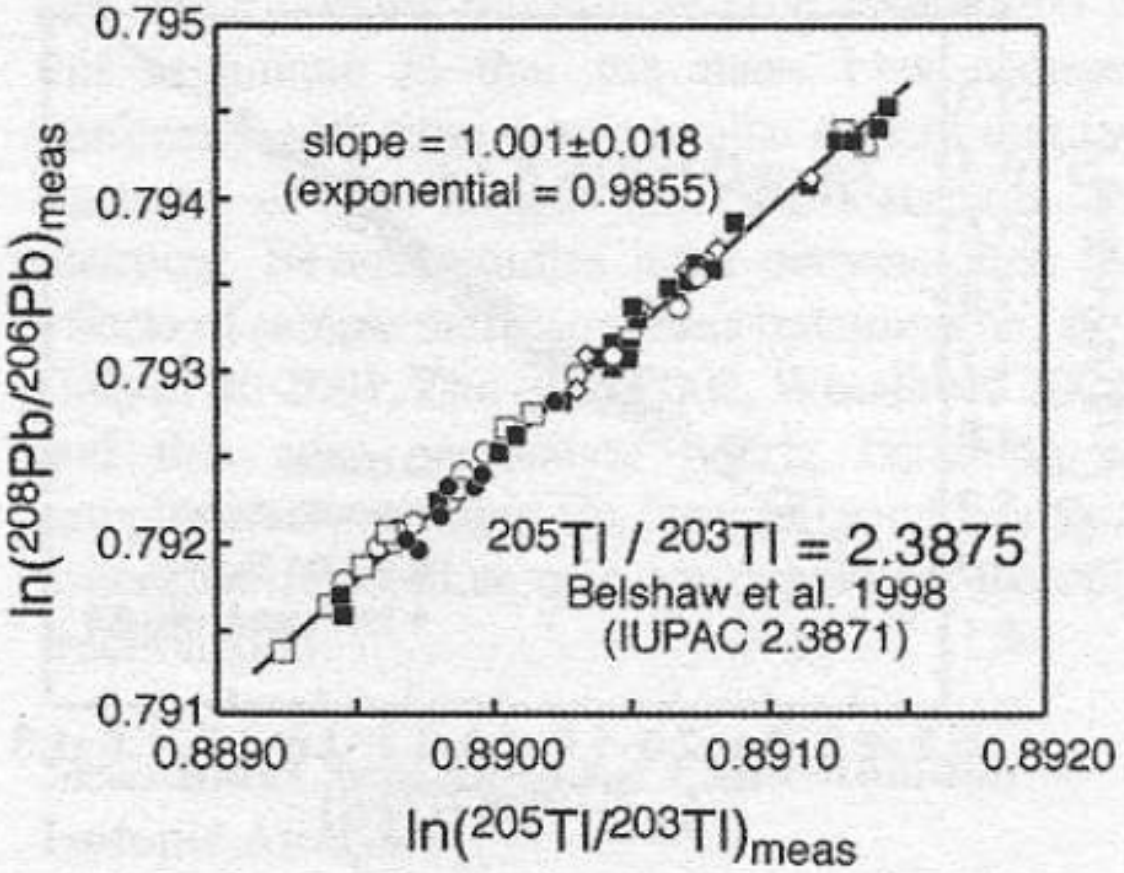

FIG. 7-4. Plot of $\ln(^{208}Pb/^{206}Pb)$ *vs.* $\ln(^{205}Tl/^{203}Tl)$ of a mixed Pb (SRM981) and Tl (SRM997) solution. The data points are from 55 analyses over a 3-year period. The slope of the line (1.001±0.018) is slightly higher than the theoretical value derived from the mass relationship of the exponential (0.9855).

Pearson et al. (2008)

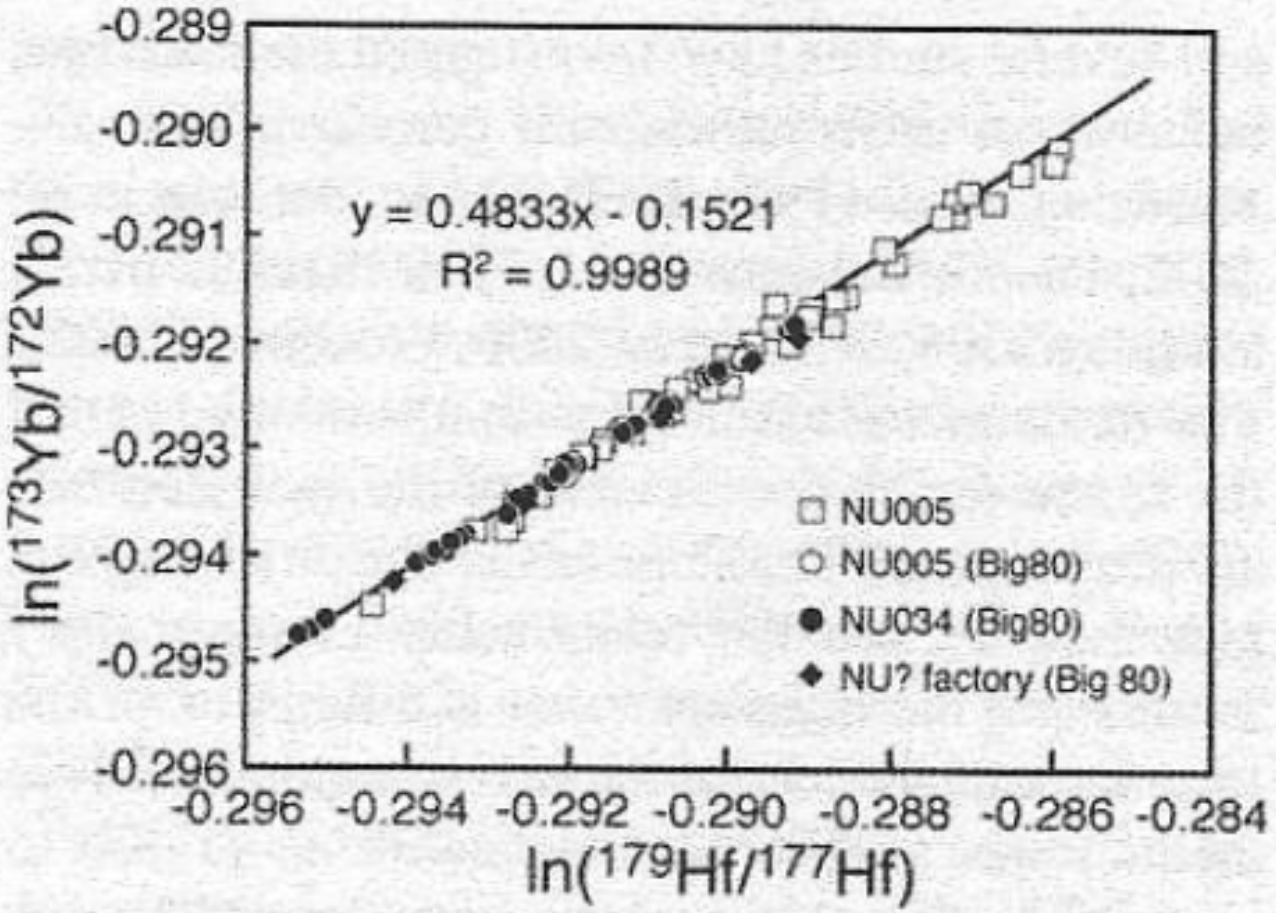

FIG. 7-5. Plot of $\ln(^{173}Yb/^{172}Yb)$ *vs.* $\ln(^{179}Hf/^{177}Hf)$ of a mixed Hf (JMC475) and Yb solution showing the similarity of mass bias behavior between three Nu Plasma MC–ICP–MS (Nu005 with and without the Big80 pump, Nu034 and Nu factory.

Pearson et al. (2008)

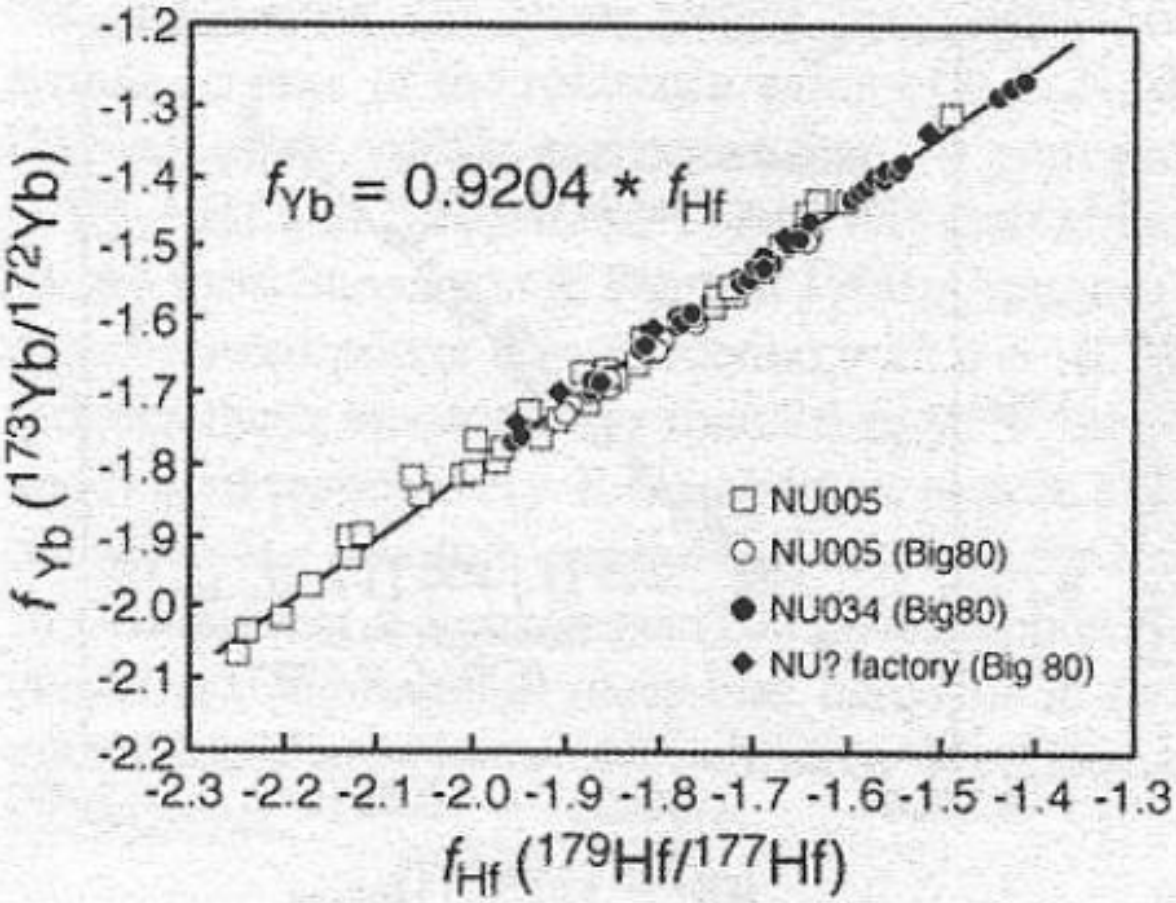

FIG. 7-6. Plot of exponential mass bias coefficient *f* for Yb ($^{173}Yb/^{172}Yb$) vs Hf ($^{179}Hf/^{177}Hf$). Data as in Fig 7-5. The linear array gives a constant relationship between *f* Hf and *f* Yb, but because the slope is not equal to one it indicates that the mass fractionations of Yb and Hf are not the same.

Pearson et al. (2008)

Instrumental Mass Bias – *Standard-Sample Bracketing*

- This method measures standards (samples) of known isotopic composition interspersed with unknown samples to monitor change in instrumental mass bias over time
- This technique is used when there are no internal isotope pairs (of constant ratio) or the addition of an external dopant (i.e., element of similar mass that is a non-isobaric overlap) is not a viable option (e.g., Li, Mg)
- The mass bias value for the unknown sample is interpolated from the inferred mass bias values obtained from a pair of standard runs (one before, and one following the sample)

Instrumental Mass Bias – *Standard-Sample Bracketing*

- Assumptions here are that:

  - the mass bias changes uniformly with time

  - matrices of sample and standard are identical; this may be of critical importance for laser ablation analyses

Instrumental Mass Bias – *Corrections*

- For accurate measurements of in-situ radiogenic isotope ratios such as $^{87}Sr/^{86}Sr$, $^{143}Nd/^{144}Nd$, and $^{176}Hf/^{177}Hf$, we need to address the issues of ***mass bias correction*** and evaluate ***isobaric interferences***

- The mass bias corrections for Sr, Nd, and Hf are relatively straightforward as each element has a pair of 'interference-free' stable isotopes that can be used for normalization
  - E.g., $^{86}Sr/^{88}Sr = 0.1194$, $^{146}Nd/^{144}Nd = 0.7219$, $^{179}Hf/^{177}Hf = 0.7325$

Instrumental Mass Bias – *Corrections*

- However, isobaric interferences in radiogenic isotope systems include:
  - $^{87}Rb \rightarrow {}^{87}Sr$ (effects $^{87}Sr/^{86}Sr$)
  - $^{144}Sm \rightarrow {}^{144}Nd$ (effects $^{143}Nd/^{144}Nd$)
  - $^{176}Lu \rightarrow {}^{176}Hf$ (effects $^{176}Hf/^{177}Hf$)
- Thus, we will discuss the various approaches that can be used to overcome the problem of mass bias correction for the isobaric interferences using the ***Lu-Hf isotope system*** as an example

Nu Plasma II Collector Configuration

	-14	-13	-12	-11	-10	-9	-8	-7	-6	-5	-4	-3	-2	-1	0	1	2	3	4	5	6	7	8	9	10	11	12
	X	F	F	X	F	X	F	X	F	F	F	F	F	F	F	F	F	F	F	F	IC0	IC1	IC2	X	IC3	X	IC4
																					Filter		Filter				
		1	2	2	3		4		5	6	7	8	9	10	11	12	13	14	15	16							
U I																			U238		U236	U235	U234				
U II																	U238			U235	U234	U233					
Th I																			Th232		Th230	Th229					
U/Th/Pb		U238					Th232														Pb208	Pb207	Pb206		Pb204		Hg202
Pb (Hg, Tl)															Pb208	Pb207	Pb206	Tl205	Pb204	Tl203	Hg202						
Pb (Hg)																	Pb208	Pb207	Pb206		Pb204		Hg202				
Hg(Tl,Pb)							Pb207		Tl205	Hg204	Tl203	Hg202	Hg201	Hg200	Hg199	Hg198	Hg197	Hg196	Pt195								
Hg(Pt,Pb)									Pb206		Hg204		Hg202	Hg201	Hg200	Hg199	Hg198	Hg197	Hg196	Pt195							
Os (W,Re,Pt)							Pt194		Os192		Os190	Os189	Os188	Os187	Os186	Re185	Os184		W182								
W(Hf,Os,Ta)									Os188		W186			W183	W182	Ta181	W180	Hf179	Hf178								
Hf(Yb,Lu,W)									W182	Ta181	Hf180	Hf179	Hf178	Hf177	Hf176	Lu175	Hf174	Yb173	Yb172	Yb171							
Lu/Er(Hf,Yb)									177Hf	Lu176	Lu175		Yb173	Yb172					Er167	Er166							
Gd (Dy,Sm)					Dy162		Gd160		Gd158	Gd157	Gd156	Gd155	Gd154		Gd152			Sm149									
Nd(Sm,Ce)									Nd150		Nd148	Sm147	Nd146	Nd145	Nd144	Nd143	Nd142		Ce140								
Ce(Nd,La,Ba,Xe)					Nd146				Ce142		Ce140	La139	Ce138	Ba137	Ce136	Ba135				Xe131							
Ba (Xe,La,Ce)											Ce140	La139	Ba138	Ba137	Ba136	Ba135	Ba134		Ba132	Xe131							
Pd(Ru,Cd,Ag)										Cd111	Pd110	Ag109	Pd108	Ag107	Pd106	Pd105	Pd104		Pd102	Ru101							
Ru(Mo,Pd)			Pd104				Ru102		Ru101		Ru100		Ru99		Ru96		Mo97		Ru96								
Mo(Zr,Ru)			Mo100		Ru99		Mo98		Mo97		Mo96		Mo95		Mo94				Mo92		Zr91						
Zr(Mo,Ru)							Zr96		Mo95		Zr94				Zr92		Zr91		Zr90								
Sr (Rb, Kr)							Sr88		Sr87		Sr86		Rb85		Sr84		Kr83										
Se (Ge, Kr)			Se82				Se80				Se78		Se77		Se76				Se74		Ge73						
Ge (Se)					Se77		Ge76				Ge74		Ge73		Ge72				Ge70								
Zn(Cu,Ni,Ge)			Zn70		Zn69		Zn68		Zn67		Zn66		Cu65		Zn64		Cu63		Ni62								
Cu												Cu65						Cu63									
Cl											Cl37								Cl35								
B					B11															B10							
C					C13															C12							
Li			Li7																	Li6							
Mg							Mg25						Mg25						Mg24								
Si							Si30						Si29						Si28								
S							S34						S33						S32								
Fe(Cr) I		Ni60					Fe58			Fe57			Fe56						Fe54			Cr53					
Fe(Cr) II				Fe58			Fe57			Fe56						Cr54			Cr53								
Ni(Fe)				Ni62			Ni61			Ni60						Fe57			Fe57								
Cr (V,Ti)							Cr54			Cr53			Cr52			Ti49			Cr50			Ti49					

Nu Plasma II -In-situ Hf, collector configuration University of Notre Dame

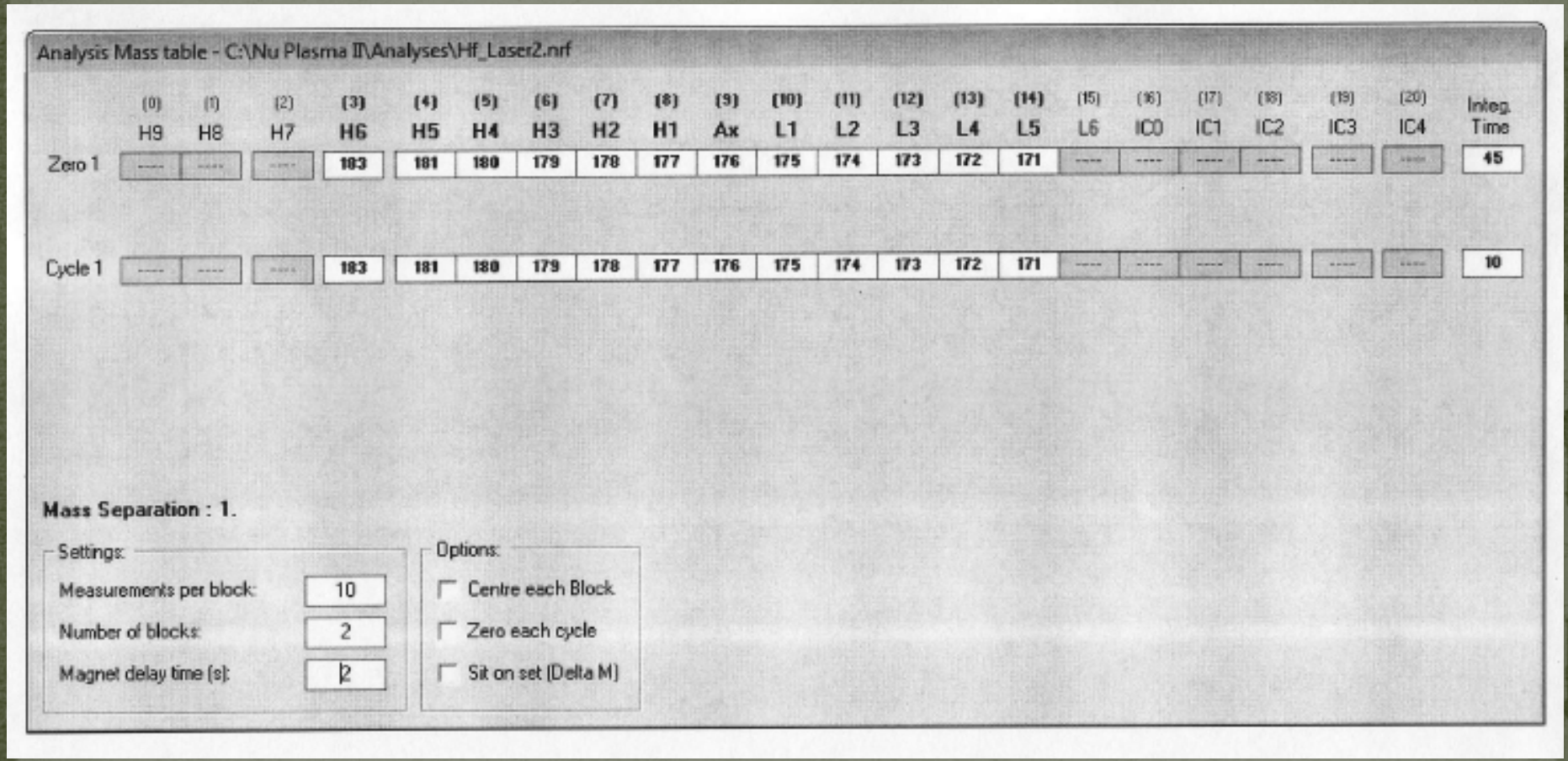

Instrumental Mass Bias – *Lu - Hf Corrections*

- **METHOD 1:**
  - Assume fHf = fLu = fYb
  - This can be evaluated by doping solutions of JMC 475 Hf standard with Yb and Lu (using desolvating nebulizing system – 'dry plasma')
  - The isotope compositions of the Yb and Lu are varied until the $^{176}Hf/^{177}Hf$ are accurate
  - Assume that mass bias for 'dry plasma' are identical as those for laser ablation analyses and instrument conditions are stable

Instrumental Mass Bias – *Lu - Hf Corrections*

- **METHOD 2:**
  - f_{Hf} , f_{Yb} are measured independently
  - Measure $^{173}Yb/^{171}Yb$, $^{172}Yb/^{171}Yb$ ratios, then assume $^{176}Yb/^{172}Yb = 0.5865$ (Segal et al., 2003)
  - Natural abundances of ^{171}Yb and ^{173}Yb are 14.28% and 16.13%, respectively. This translates into low ion signals (≤ 20 millivolts)
  - Hence, the uncertainty associated with the measurement in the f_{Yb} will affect and contribute to the uncertainty on the corrected $^{176}Hf/^{177}Hf$ ratio

Instrumental Mass Bias – *Lu - Hf Corrections*

- **METHOD 2:**
  - Wu et al. (2006) adopted using the mean $^{173}Yb/^{171}Yb$ ratio to calcuate the mean f_{Yb} for each analysis, and they showed a two-fold improvement in the precision of the $^{176}Hf/^{177}Hf$ isotope measurements.

Instrumental Mass Bias – *Lu - Hf Corrections*

- **METHOD 3:**

  - $f_{Lu} = f_{Yb}$

- Assume a constant relationship between the f_{Lu} and f_{Yb} over a long period of time and between different types of analyses (both 'dry plasma' vs. laser ablation modes)

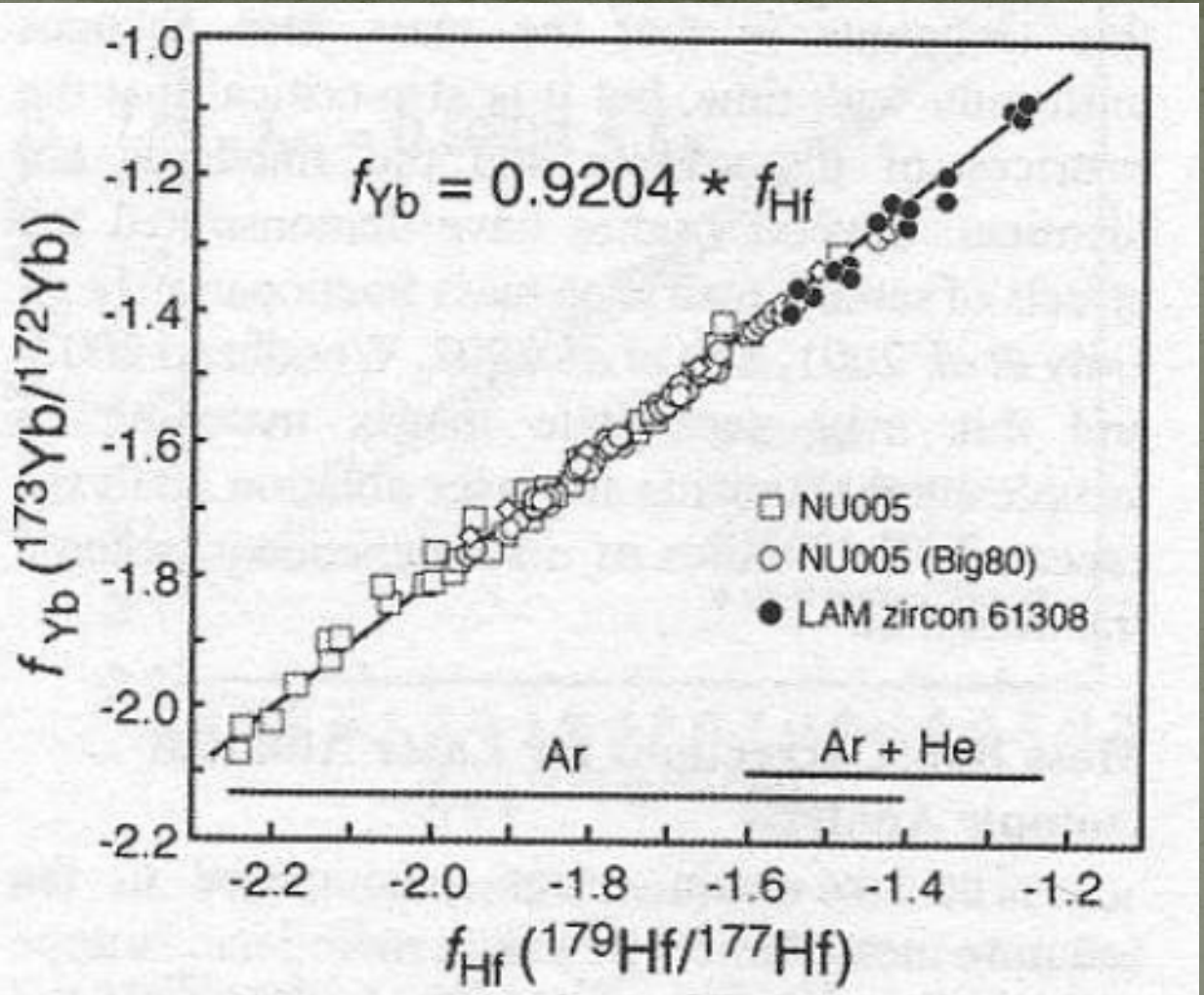

FIG. 7-7. Plot of exponential mass bias coefficient *f* for Yb (^{173}Yb/^{172}Yb) *vs.* Hf (^{179}Hf/^{177}Hf) showing results for solution analysis (data as in Fig. 7-6) and laser ablation analysis of reference zircon standard 61308.

Pearson et al. (2008)

Mass Bias – Correction Methods Summary

- Choice of method for the correction of an isobaric overlap requires careful assessment of the mass bias both in terms of within-run variations, analytical precision, and longer term instrument stability

- In order to do this, it is important to consider the factors that control instrumental mass bias

Factors Contributing to Instrumental Mass Bias

- Fundamental previous studies have shown that mass bias is generated within the plasma, within the interface region (between sample and skimmer cones), and immediately behind skimmer cone
- Physical properties of the plasma control the vaporization, atomization and ionization of the sample
- Parameters such as gas kinetic temperature and electron density parameters have a significant effect on diffusion rates in the ICP and kinetic energy of the ion transmitted through the interface

Factors Contributing to Instrumental Mass Bias

- It is commonly accepted that only ions from the central channel of the plasma can be effectively sampled into the mass spectrometer
- Processes that result in preferential vaporization of light isotopes from dry aerosol particles or mass-dependent diffusion contribute to mass bias and element fractionation
- Temperature in central channel and in front of the sample cone orifice is critical to the degree of ionization

Space charge effects

The mutual repulsion of ions of like (similar) charge limits the total number of ions that can be compressed into a beam of given size

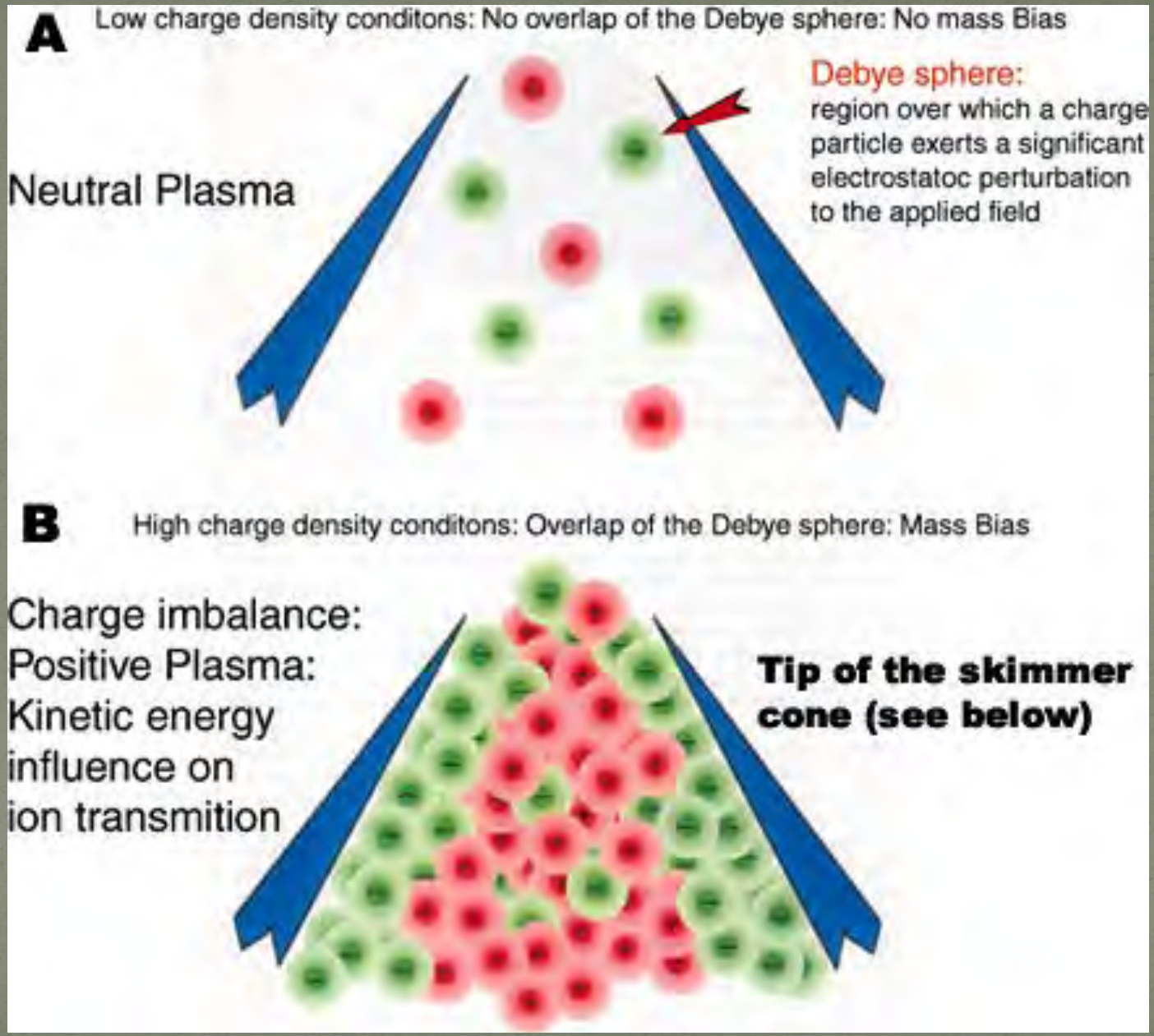
A
Low charge density conditons: No overlap of the Debye sphere: No mass Bias
Neutral Plasma
Debye sphere:
region over which a charge particle exerts a significant electrostatoc perturbation to the applied field
B
High charge density conditons: Overlap of the Debye sphere: Mass Bias
Charge imbalance:
Positive Plasma:
Kinetic energy influence on ion transmition
Tip of the skimmer cone (see below)

Factors Contributing to Instrumental Mass Bias

- Which instrument operating parameters exert an important control on the mass bias?
  - vs.
- Those produced by the laser ablation process itself (plasma loading)?

Factors Contributing to Instrumental Mass Bias

- Instrumental parameters that effect instrumental mass bias include:
  - Nebulizer gas flow
  - Extraction lens voltage
  - RF power
  - Torch Depth Position
  - Cone design and condition
  - Nebulizer gas composition

Extraction Voltage

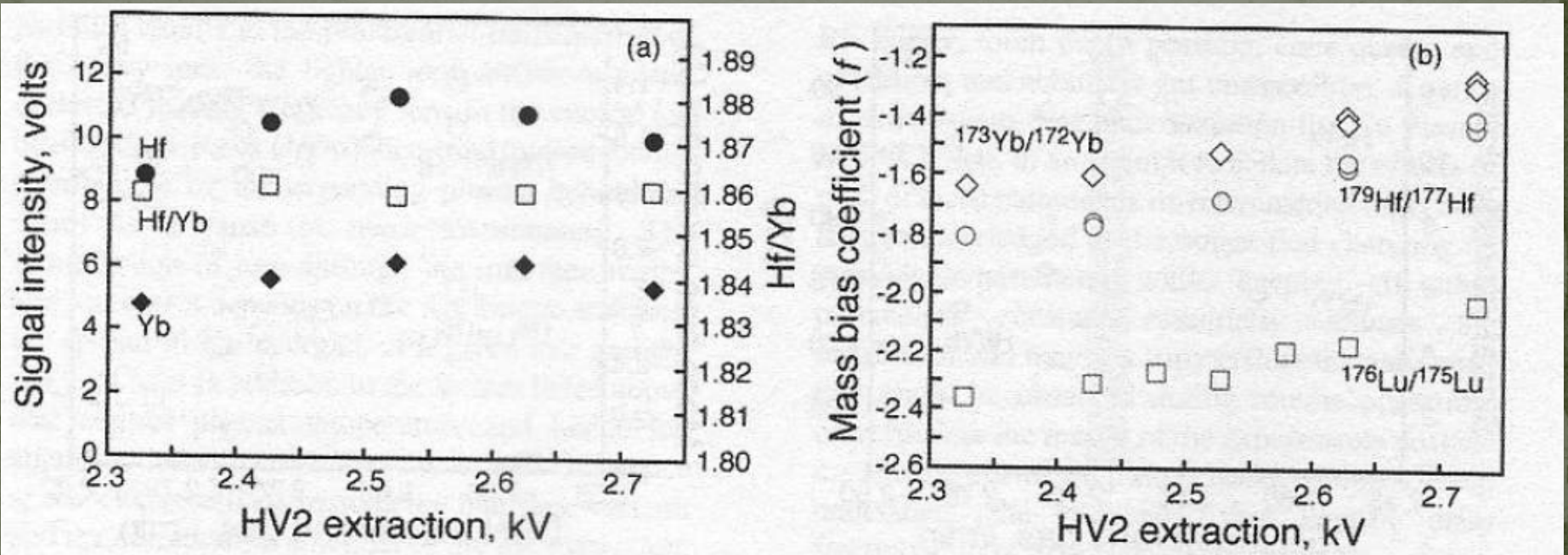

FIG. 7-10. (**a**) Plot of Hf and Yb sensitivity (volts), and Yb/Hf ratio *versus* HV2 extraction lens voltage (kV) for a mixed Yb–Hf solution; (**b**) Plot of exponential mass bias coefficient *f* for Yb ($^{173}Yb/^{172}Yb$) and Hf ($^{179}Hf/^{177}Hf$) *versus* HV2 extraction lens voltage (kV).

Pearson et al. (2008)

Torch Depth

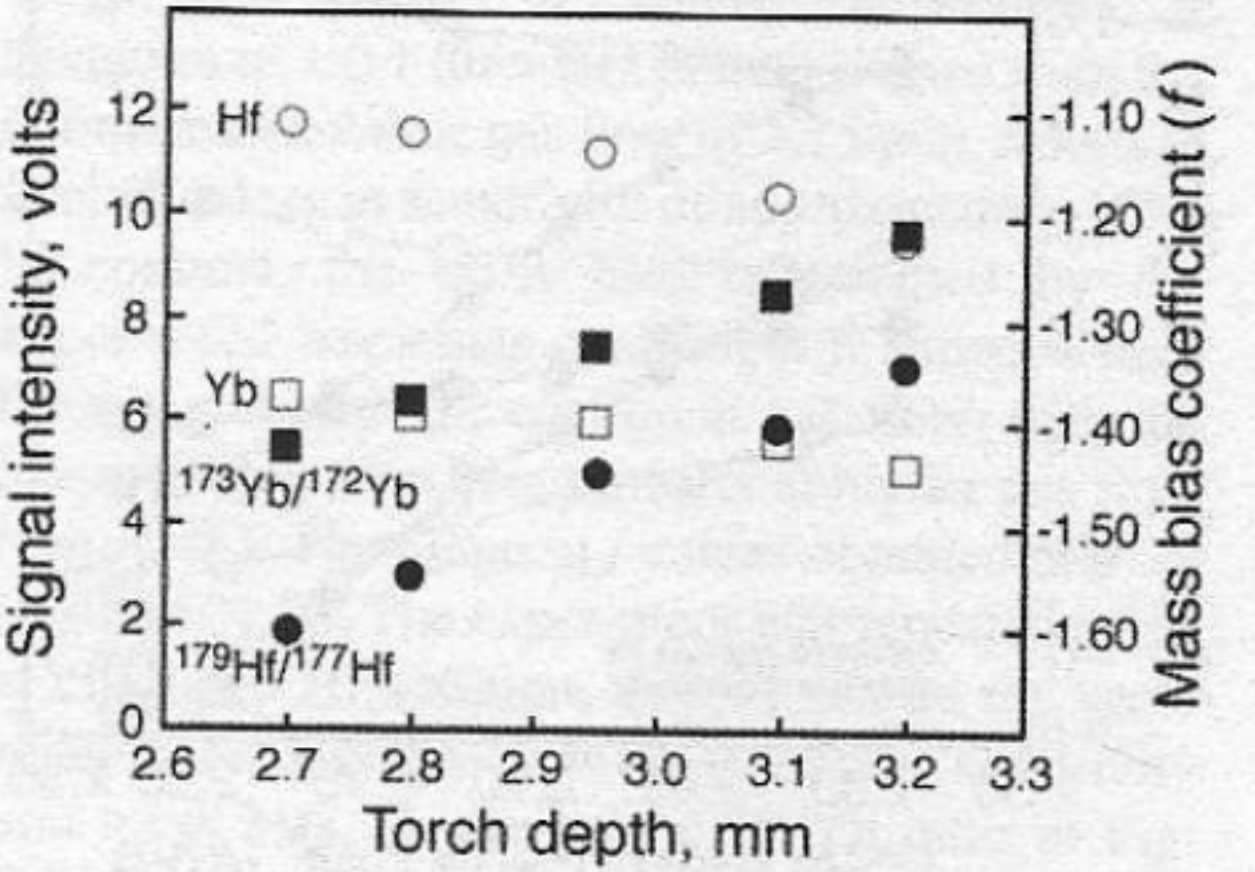

FIG. 7-11. Plot of signal intensity (volts) and exponential mass bias coefficient f for Yb ($^{173}Yb/^{172}Yb$) and Hf ($^{179}Hf/^{177}Hf$) *versus* torch depth for a mixed Yb–Hf solution.

Pearson et al. (2008)

RF Power

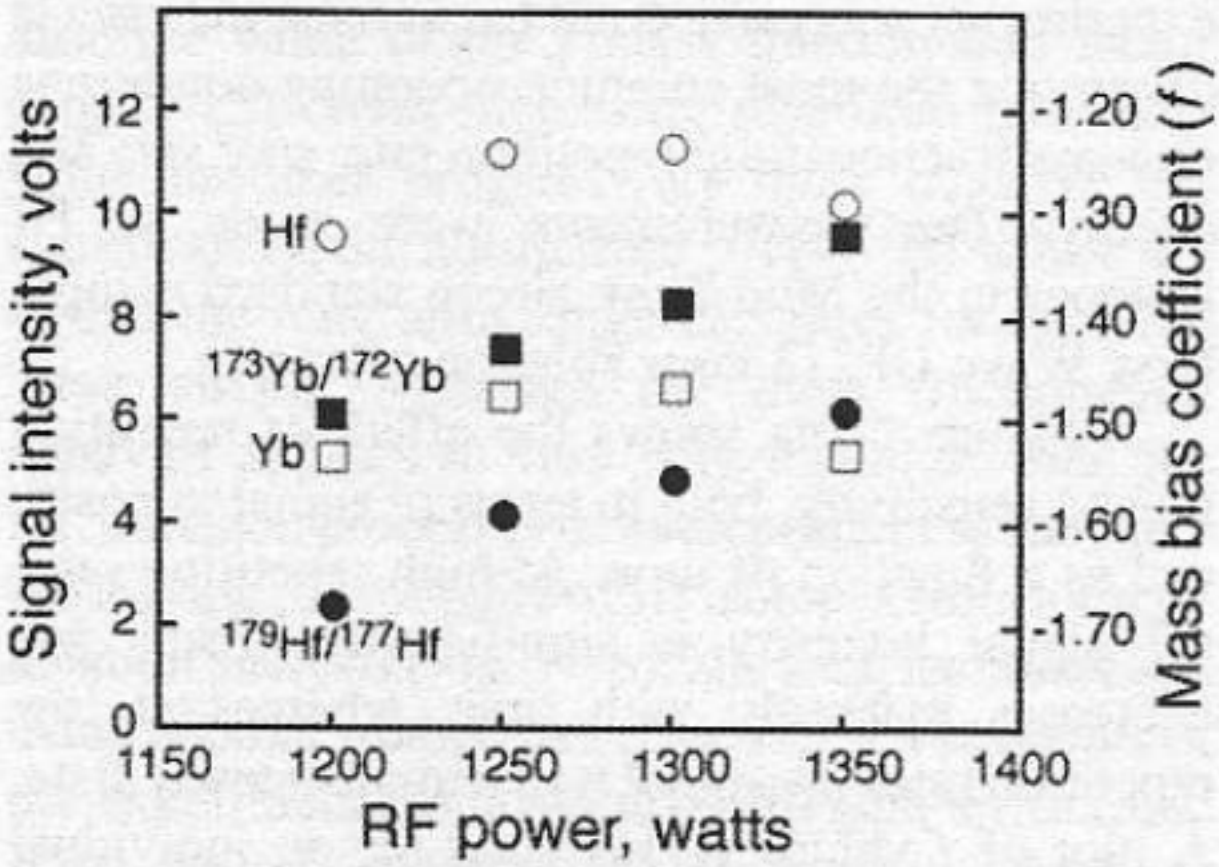

FIG. 7-12. Plot of signal intensity (volts) and exponential mass bias coefficient *f* for Yb ($^{173}Yb/^{172}Yb$) and Hf ($^{179}Hf/^{177}Hf$) *versus* forward RF power (watts) for a mixed Yb–Hf solution.

Pearson et al. (2008)

TABLE 7–1: COMPARISON OF AVERAGE MASS BIAS COEFFICIENTS FOR HF OBTAINED BY SOLUTION ANALYSIS USING A DESOLVATION NEBULIZER AND LASER ABLATION.

	n	*f*(Hf)	2σ
JMC475			
NU005 standard skimmer	79	–1.987	0.285
NU005 Wide angle skimmer	190	–1.683	0.222
NU005 Big80	110	–1.686	0.160
LAM zircon			
NU005 standard skimmer	1295	–2.052	0.319
NU005 Wide angle skimmer	14061	–1.464	0.310
NU005 Big80	12211	–1.522	0.267

Pearson et al. (2008)

Factors Contributing to Instrumental Mass Bias

- **Laser Induced Isotopic Fractionation:**
  - Particle size distribution is important – incomplete ionization of larger particles in the plasma results in increased transmission of lighter isotopes (Jackson & Günther, 2003; Kühn et al., 2007, Günther & Koch, 2008)
  - Although the laser is controlling the particle size distribution, the isotopic fractionation is occurring within the plasma

Factors Contributing to Instrumental Mass Bias

- **Laser Induced Isotopic Fractionation:**
  - Intrinsic physics of the laser design and operating conditions are considered to be the most important factors that contribute to LIEF
  - Laser pit width, wavelength, repetition rate, and energy density
  - Experiments conducted using UP213 laser ablation system and Mud Tank zircon

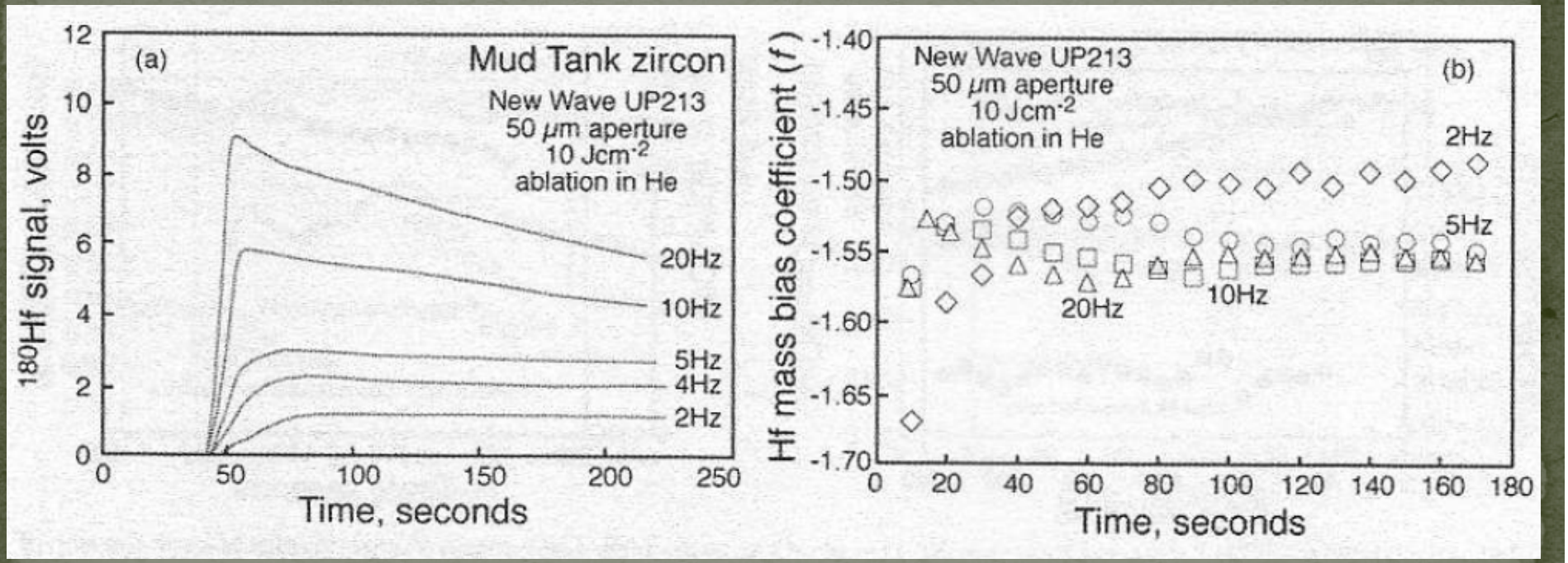

Pearson et al. (2008)

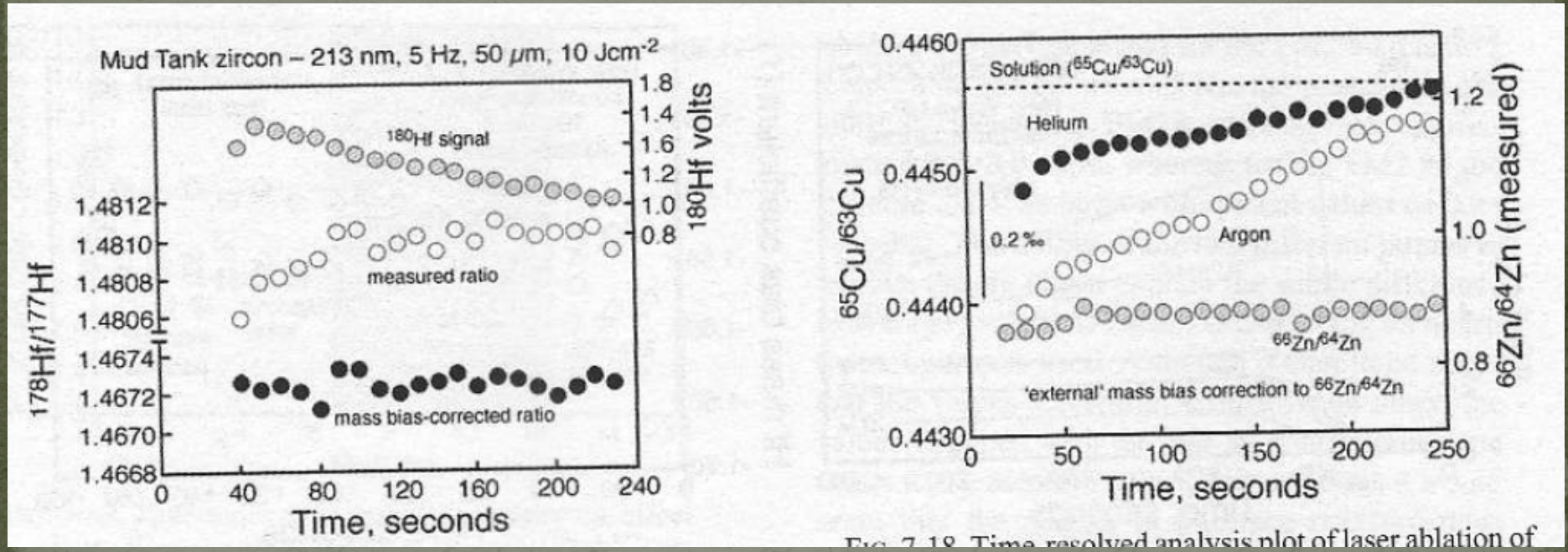

Fig. 7.18. Time-resolved analysis plot of laser ablation of

Pearson et al. (2008)

Factors Contributing to Instrumental Mass Bias

- **Laser Induced Isotopic Fractionation:**
  - "**Mass (Plasma) Loading**" – amount of material introduced into the ICP, has been shown to have a large effect on elemental fractionation
  - The influence of plasma loading can be evaluated in a plot of mass bias coefficient '*f*' versus total ion signal (volts)
  - Hopefully, you will not see a correlation between *f* and the corrected isotope ratios of interest!

Factors Contributing to Instrumental Mass Bias

- **Laser Induced Isotopic Fractionation:**
  - "**Matrix Effects**" – Several previous studies indicate there is an important effect of the sample matrix on the observed mass bias
  - However, Pearson et al. (2008) clearly show that although different concentrations of matrix elements clearly effect the calculated mass bias coefficient "f", the varying matrix conditions did not have an impact on the calculated isotope ratio of interest!

SUMMARY

- There are 3 categories of factors that effect the accuracy and precision of in situ isotope ratio measurements by LA-MC-ICP-MS:
  - SAMPLE
  - MASS SPECTROMETER
  - LASER ABLATION SYSTEM

SUMMARY

- **Accuracy** is mainly a function of:
  - Correction procedures for mass bias
  - Isobaric interferences
  - Sample matrix effects

- Precision is a function of:
  - Ion signal intensity – which is dependent on concentration of element in sample, laser energy, spot size, mass spectrometer sensitivity, and time of laser ablation analysis

SUMMARY

- Correction for mass-dependent instrumental mass bias '*f*' is the most critical factor controlling the **accuracy**!!

- Instrument operation parameters that affect mass bias for in-situ laser ablation analysis include:
  - Nebulizer gas flow rate
  - RF power
  - Voltages, torch position, and cone design
  - Matrix (sample-related)
  - Laser operating conditions

SUMMARY

- The interplay of all these factors that influence the accuracy and precision emphasizes the need for ***reference materials*** that are well characterized, in terms of their **isotopic composition** AND their **major and trace element constituents**

In-situ Nd isotope Studies - LA-MC-ICP-MS

Applications

- Trace ancient crustal differentiation events
- Hydrothermal activity/diagenetic processes
- Trace magmatic/mantle processes

Background

- Nd isotope analyses by ID-TIMS (isotope dilution-thermal ionization mass spectrometry) using whole rocks generates high precision results; however, isotopic heterogeneities at the scale of ***individual minerals*** is lost

- However, compared to a ID-TIMS analysis, 1000 times less sample is consumed for a typical LA-MC-ICP-MS result, therefore application of this method is dictated by the absolute concentrations of Nd (ppm) in the sample

Background

- Hence, the in-situ Nd isotopic method is applicable to LREE- enriched accessory minerals – most notably
  - Monazite, allanite, titanite, and ***apatite***

Background

- Naturally, the interesting aspect of applying the in-situ Nd isotope technique to minerals such as apatite and monazite, is that you can also obtain in-situ U-Pb ages for these phases

- Hence, this combination of U-Pb ages and Nd (Sr, Pb) isotope ratios becomes a powerful technique for tracing a variety of igneous processes

$$^{143}Nd/^{144}Nd = {}^{143}Nd/^{144}Nd_o + {}^{147}Sm/^{144}Nd\ (e^{\lambda t} - 1)$$

^{147}Sm decays to ^{143}Nd

$\lambda = 6.54 \times 10^{-12}$

Analytical Challenges

- 1- Removal of the isobaric interference of ^{144}Sm on ^{144}Nd
- Assessing the accuracy of corrected ratios
- Obtaining an accurate $^{147}Sm/^{144}Nd$ ratio

TABLE 8-1. NEPTUNE MC–ICP–MS COLLECTOR CONFIGURATION FOR ND AND SR ISOTOPE MEASUREMENTS

(a) Nd configuration and *potential* interferences

Cup	L4	L3	L2	L1	Ax	H1	H2	H3	H4
Amplifier	5	9	1	3	8	7	2	6	4
Analyte	^{142}Nd	^{143}Nd	^{144}Nd	^{145}Nd	^{146}Nd	^{147}Sm	^{149}Sm	^{153}Eu	^{155}Gd
	^{142}Ce		^{144}Sm						*$^{139}La^{16}O$*
Interferences					*$^{130}Ba^{16}O$*				
			$^{130}Ba^{14}N$		*$^{132}Ba^{14}N$*	*$^{133}Cs^{14}N$*			
		$^{103}Rh^{40}Ar$	*$^{104}Pd^{40}Ar$*	*$^{105}Pd^{40}Ar$*	*$^{106}Pd^{40}Ar$*				

(b) Sr configuration and monitored interferences

Cup	L4	L3	L2	L1	Ax	H1	H2	H3	H4
Amplifier	7	6	1	3	2	5	8	9	4
Analyte	^{83}Kr	^{167}Er^{++}	^{84}Sr	^{85}Rb	^{86}Sr	^{173}Yb^{++}	^{87}Sr	^{88}Sr	^{177}Hf^{++}
	^{166}Er^{++}		^{168}Er^{++}	^{170}Er^{++}					
			^{84}Kr		^{86}Kr				
Interferences			^{168}Yb^{++}	^{170}Yb^{++}	^{172}Yb^{++}		^{174}Yb^{++}	^{176}Yb^{++}	
							^{174}Hf^{++}	^{176}Hf^{++}	
							^{87}Rb		

Potential interferences are shown in italics.

McFarlane & McCulloch (2008)

Sm Interference Corrections

- Sm/Nd ratios in REE-bearing accessory minerals can be quite variable but typically vary between 0.05 (monazite, allanite) to 1.0 (xenotime)
- Always have isobaric interference of ^{144}Sm on ^{144}Nd, thus no choice but to strip this overlap in order to obtain accurate $^{143}Nd/^{144}Nd$ ratios

Sm Interference Corrections

- However, Sm correction is complicated since the $^{146}Nd/^{144}Nd$ ratio is used for the internal normalization, which is also affected by the interference

Sm Interference Corrections

- This interference can be addressed in several ways:
- 1- by using an iterative approach as outlined by Foster & Vance (2006);
- 2- using $^{146}Nd/^{145}Nd$ (normalized to $^{146}Nd/^{144}Nd$ measured using pure Nd solutions)
- 3- Monitoring an additional interference free invariant ratio such as $^{147}Sm/^{149}Sm$ to correct $^{144}Sm/^{149}Sm$ – then applying this to the $^{146}Nd/^{144}Nd$ for mass bias correction purposes (McFarlane & McCulloch, 2007)

Sm Interference Corrections

Iterative approach - Foster & Vance (2006);

- Use the NIST SRM 610 international glass standard to establish $^{144}Sm/^{147,149}Sm$ working values in order to obtain the appropriate Nd isotope values
- Isotopic homogeneity of reference standard is critical, especially for samples with Sm/Nd >0.1

Sm Interference Corrections

McFarlane & McCulloch (2007)

- Invariant ratios for Sm ratios were measured with pure Sm solutions
- Interference of ^{144}Sm on ^{144}Nd is then corrected by monitoring ^{149}Sm and using a value for $^{144}Sm/^{149}Sm$ obtained by doping Nd standard solutions with variable Sm contents and iteratively refining the $^{144}Sm/^{149}Sm$ to give the true Nd isotope values

TABLE 8-2. REE AND TRACE-ELEMENT CHEMISTRY OF NATURAL ACCESSORY MINERALS

	Trebilcock monazite		Daibosatsu allanite		Fish Canyon Tuff titanite		*Durango apatite		†Phalabowra apatite	
	(n = 20)		(n = 20)		(n = 10)		(n = 30)		(n = 5)	
(ppm)	Mean	1σ	Mean	1σ	Mean	1σ	Mean	1σ	Mean	1σ
Be	0.06	0.06	0.53	0.07	0.01	0.01	-	-	<0.01	
As	311	27	93.4	20.6	36.2	13.1	802	23	18.1	2.3
Rb	2.02	0.1	0.7	0.1	1.15	0.5	0.06	0.01	0.04	0.0
Sr	2.30	0.7	2.0	0.5	27.0	9.3	475	11	4685	59
Y	21130	148	4273	551	5098	2005	456	13	191	18
Pd	<0.01	-	<0.01	0.0	0.02	0.00	-	-	<0.01	-
Cd	-	-	-	-	-	-	<0.12	-	-	-
Cs	<0.01	-	<0.01	-	0.03	0.01	<0.07	-	<0.01	-
Ba	0.16	0.05	<0.03	-	0.05	0.04	1.44	0.06	74.5	2.9
La	63146	5833	56122	3024	3179	337	3370	87	1139	132
Ce	154722	1420	104506	5909	11063	1007	4282	116	2803	295
Pr	20893	1874	8494	401	1660	299	336	9	372	38
Nd	87868	7925	24397	716	7390	2000	1040	29	1581	154
Sm	32559	2341	3191	99	1576	652	127	3.3	266	25
Eu	157	8.3	4.1	1.5	168	45	15.3	0.4	54.0	5.3
Gd	21011	1054	1902	81	1174	535	109	3.2	166	16
Tb	2649	88	237	17	183	88	12.9	0.4	16.1	1.6
Dy	8726	172	1085	108	1047	492	73.9	3.0	60.2	5.7
Ho	800	5.9	165	19	199	87	14.3	0.5	7.73	0.7
Er	1090	18	349	48	505	201	38.6	1.3	13.3	1.4
Tm	93	2.6	42	6.3	69	24	4.9	0.2	1.17	0.1
Yb	395	14	267	41	436	123	27.8	0.9	5.41	0.6
Lu	28	1.3	33	4.8	49	11	3.65	0.1	0.60	0.1
Pb	802	87	5.3	0.3	1.74	0.14	0.53	0.0	79.5	15
Th	144085	2026	7893	1625	259	60	181	8.6	295	53
U	15827	1763	615	58	147	28	8.88	0.4	60.3	15
Sm/Nd	0.371		0.131		0.213		0.122		0.169	
$^{147}Sm/^{144}Nd$	0.234		0.082		0.134		0.077		0.106	

*Data from Trotter & Eggins, 2006; †Preliminary values

McFarlane & McCulloch (2008)

TABLE 8-3. POTENTIAL ND AND SR ISOTOPE MINERAL STANDARDS

(a) Sm-Nd isotope reference material

Standard	Age (Ma)	Rock type	Nd (ppm)	$^{147}Sm/^{144}Nd$ (2σ)	$^{143}Nd/^{144}Nd$ (2σ)	Notes
Trebilcock monazite, Maine	270	Granitic pegmatite	~98000	0.2322 (16) 0.2313 (10) 0.234	0.512593 (3)* 0.512586 (8)* 0.512623 (1)†	2006-2008 ANU average, *n* = 33 June 2008 MUN, *n* = 11 Tomascak et al., (1998)
Daibosatsu allanite, Japan	13	Granitic pegmatite	~25000	0.0840 (8) 0.0810 (20)	0.512569 (3)* 0.512577 (10)* 0.512558 (8)**	2006-2008 ANU average, *n* = 23 June 2008 MUN, *n* = 10 McFarlane & McCulloch (2007)
Siss3 allanite, Bergell intrusion	34	Tonalite	~18600	0.1300	0.512352 (5)†	von Blanckenburg et al. (1992)
Fish Canyon Tuff titanite, Colorado	28	Felsic tuff	~7400	0.1246 (80) 0.1143 (66)	0.512170 (5)* 0.512171 (10)* 0.512171 (16)**	2007 ANU average, *n* = 17 June 2008 MUN, *n* = 4 This study, multi-grain fraction
Fish Canyon Tuff apatite, Colorado	28	Felsic tuff	~1400	0.0876	0.512213 (8)**	Foster & Vance (2006)
Durango apatite, Mexico	31	Fumarolic cavities	~1000 ~1600	0.0763 (14) 0.0765 (5) 0.0867	0.512449 (10)* 0.512469 (16)* 0.512483 (4)**	2007 ANU average, *n* = 10 June 8 MUN, *n* = 7 Foster & Vance (2006)

(b) Sr-isotope reference material for apatite

			Sr (ppm)	$^{87}Rb/^{86}Sr$	$^{87}Sr/^{86}Sr$	
Durango apatite	31		~475	<0.0001	0.70629 (2)†	2007 ANU Triton
Phalabowra apatite	2060	Pegmatite	~4500	<0.0001	0.70738 (3)†	2007 ANU Triton

*analyzed by LA-MC-ICPMS; **analyzed by solution-MC-ICPMS; †analyzed by TIMS; MUN, Memorial Univ. of Nfld.

McFarlane & McCulloch (2008)

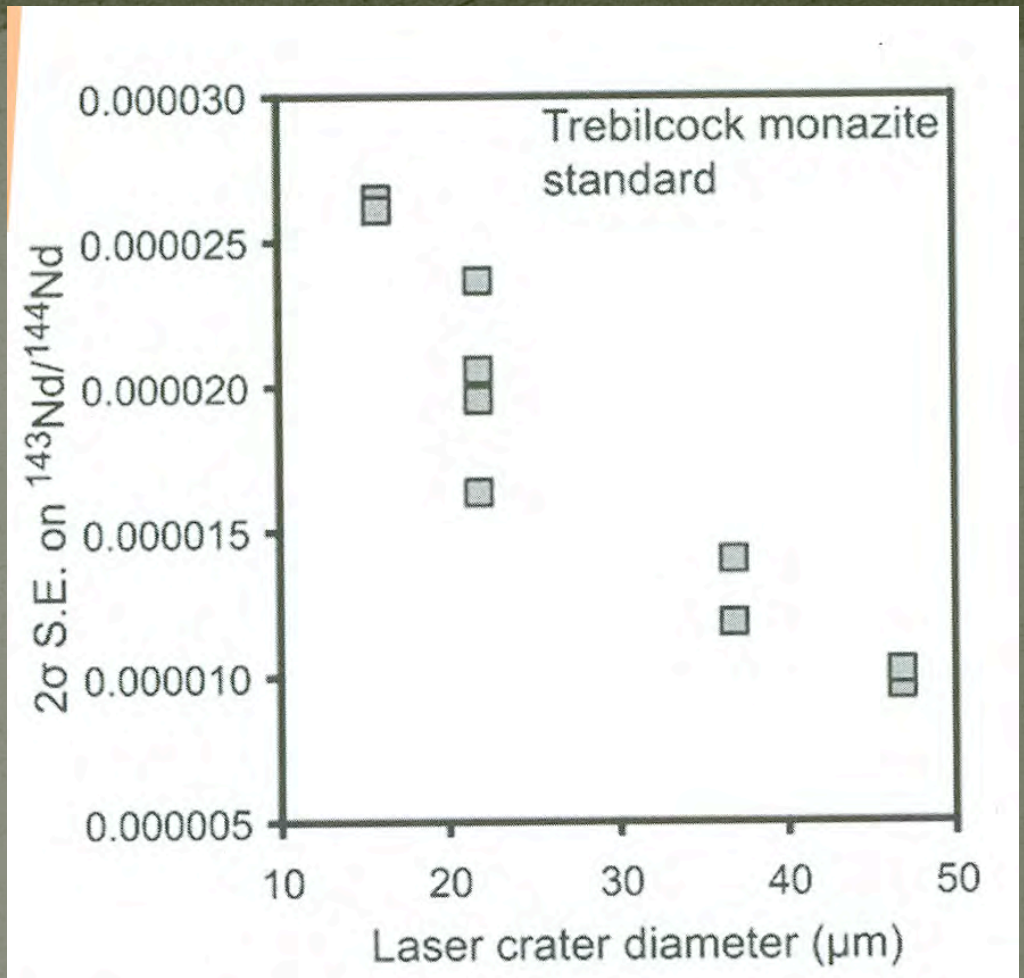

FIG. 8-1. Effect of increasing laser crater diameter on 2σ standard error for $^{143}Nd/^{144}Nd$ as measured on the Trebilcock monazite standard. The high Nd concentration of monazite (typically >9 wt.% Nd) allows high precision measurements to be obtained even for laser crater diameters of < 20 μm. TIMS-level (*e.g.*, <10 ppm) precision can be obtained on monazite for laser crater diameters of ~ 50μm

McFarlane & McCulloch (2008)

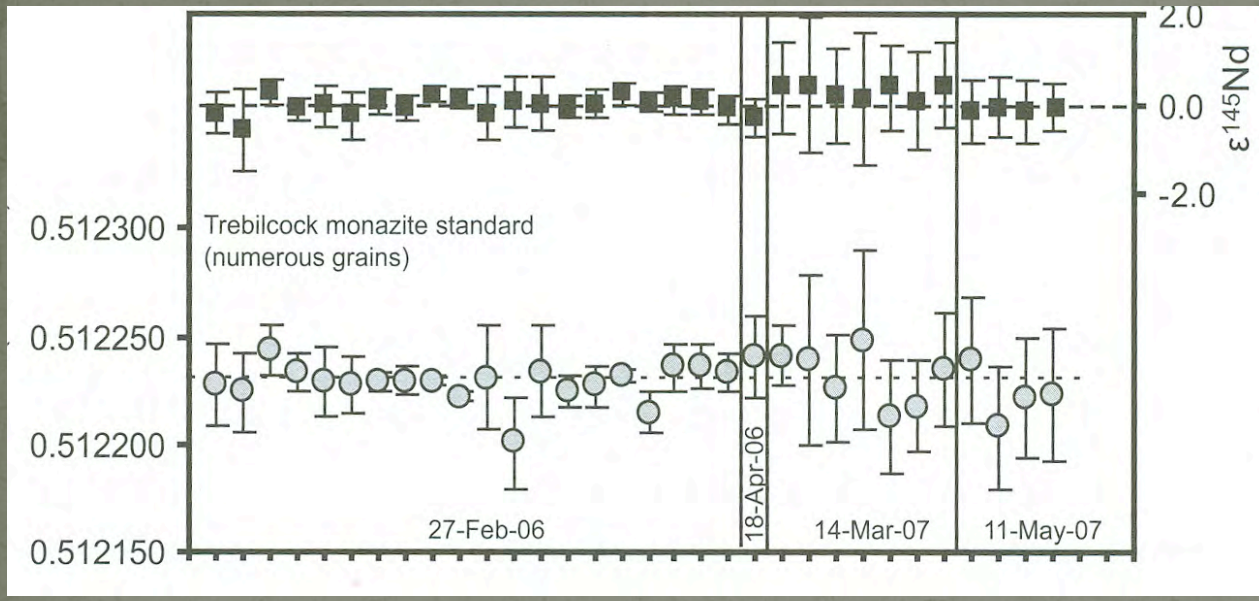

FIG. 8-2. Long term (2 year) internal ($\varepsilon^{145}Nd$) and external (initial $^{143}Nd/^{144}Nd$) reproducibility measured on numerous different grains of Trebilcock monazite liberated from a single large translucent fragment. The size of 2σ error bars in inversely proportional to laser crater diameter (see Fig. 8-1).

McFarlane & McCulloch (2008)

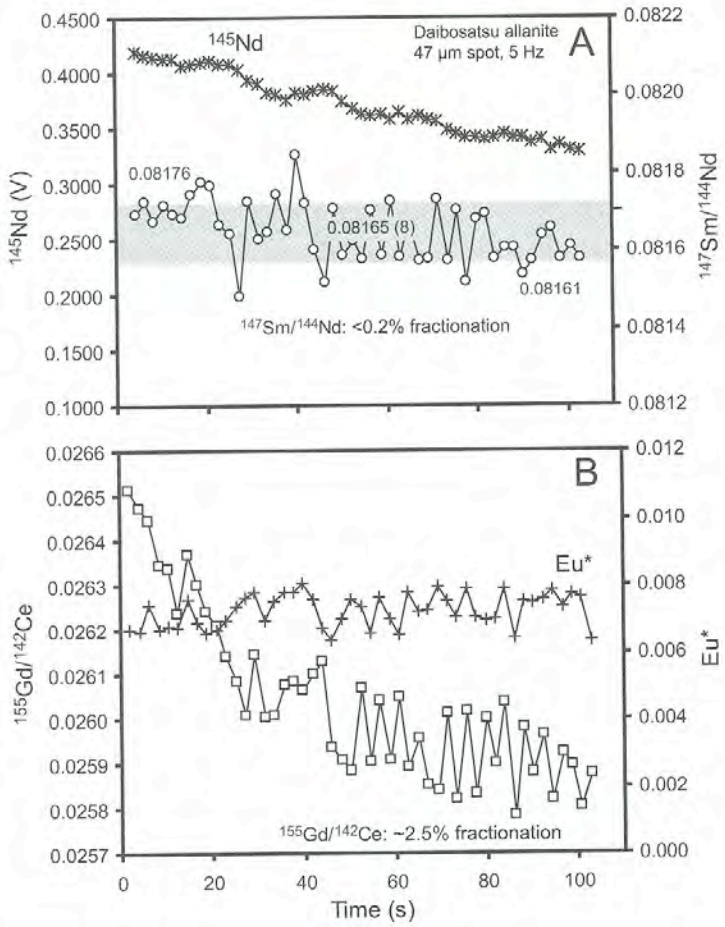

FIG. 8-3. Laser-induced time-dependent behavior measured on a chemically and isotopically homogeneous grain of Daibosatsu allanite. A) Deepening of the laser crater leads to a monotonic decrease in ion beam intensity as monitored by ^{145}Nd and a <0.2% fractionation of $^{147}Sm/^{144}Nd$. This level of fractionation is typically much smaller than natural intragranular zoning in Sm/Nd. B) As expected $^{155}Gd/^{142}Ce$ displays a significantly larger time-dependent fractionation of ~2.5%. The constant Eu* also attests to the chemical homogeneity of the target.

McFarlane & McCulloch (2008)

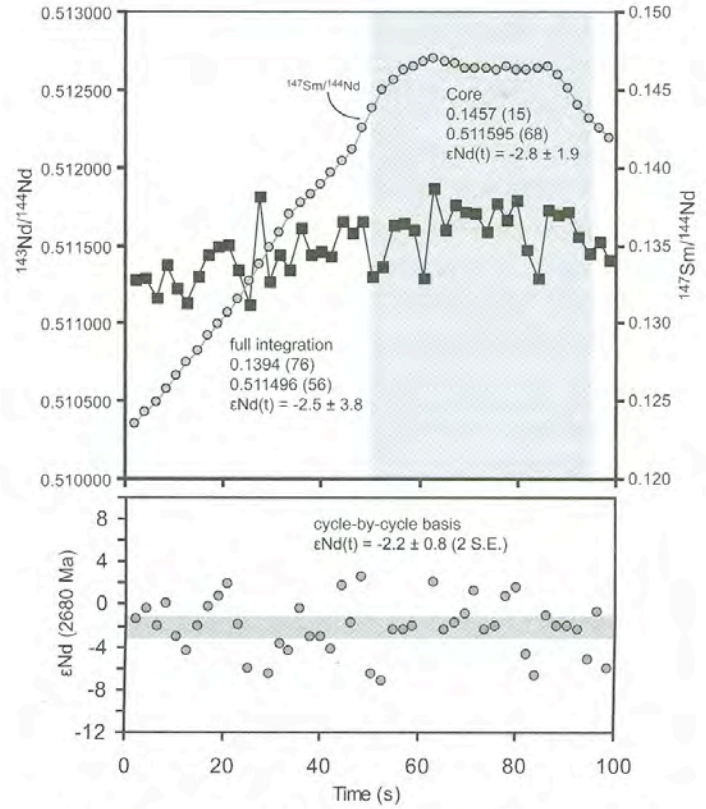

FIG. 8-4. Time series for a 2.68 Ga allanite grain from the Teton Ranges showing intracrystalline chemical and isotopic heterogeneity. The grain displays a discrete core as recorded by $^{147}Sm/^{144}Nd$. The corrected $^{143}Nd/^{144}Nd$ also displays a monotonic increase approaching the core the mimics the increasing $^{147}Sm/^{144}Nd$ ratio. Full integration of the time series yields a weighted mean 147Sm/144Nd with a ~5.5$ error that compromises the precision on the calculated εNd(t) value. A better estimate of εNd(t) can be obtained by either limiting the integration to the core region or by calculating εNd(t) on a cycle by cycle basis (as shown in lower panel) and taking the mean for this population. Both methods yield more precise and accurate εNd(t) values that overlap within error.

McFarlane & McCulloch (2008)